Tearing instability in polypropylene

K. Prabhat and J. A. Donovan
Mechanical Engineering, University of Massachusetts, Amherst, MA 01003, USA
(Received 11 January 1985)

Polypropylene can fail by tearing instability when the elastic contraction is greater than the plastic extension due to crack growth. Tearing instability theory developed by Paris and co-workers describes the effect of specimen geometry on the ductile fracture properties of polypropylene. Crack growth in compact tension specimens was always stable, but the stability of crack growth in double edge notched and three point bend specimens depended on the specimen's dimensions.

(Keywords: *J*-integral; ductile fracture; tearing instability; geometry effects; strain rate; polypropylene)

INTRODUCTION

Polymeric materials are increasingly being used for load bearing structural applications and, therefore, understanding their fracture properties is becoming more important. Linear elastic fracture mechanics (LEFM) has successfully described the fracture properties of brittle polymers, e.g. polypropylene (PP) below its glass transition temperature[1,2]. However, many polymers of great engineering interest are ductile and predictions of failure based on LEFM can be extremely conservative for these materials, such as polyethylene and PP. Significant progress has been made in characterizing the initiation of crack growth in ductile materials, primarily metals, in terms of the *J*-integral concept discovered by Rice[3] and suggested by Begley and Landes[4] as a fracture criterion that has resulted in a standard procedure[5]. Recently Hodgkinson and Williams[6] successfully described the initiation of ductile fracture in polyethylene by the *J*-integral.

The *J*-integral may be interpreted in two ways: (a) the intensity of the elastic–plastic deformation and stress field in the crack tip region or (b) the change in energy of the cracked body due to a small extension of the crack. However, since sustained crack growth in ductile materials requires additional energy, even the *J*-integral value for initiation is conservative in describing the fracture resistance and only describes the initiation of crack growth. Therefore, the *J* resistance curve (*J versus* change in crack length) is commonly used to characterize the crack extension behaviour of ductile materials.

Paris *et al.*[7] have extended this approach to characterize the conditions for crack instability in a ductile material in terms of a non-dimensional parameter, *T*, the tearing modulus.

The objective of this study was to determine if the theory of tearing instability (TIS) based on the *J* integral could explain the results of Gotham and Scrutton[8], who reported that the fracture of PP at room temperature depended on specimen type. Specifically, they found a centre cracked specimen failed in a brittle manner, but a cracked compact tension specimen failed in a ductile manner at the same temperature and strain rate. They therefore concluded that life size specimens need to be tested in order to determine the failure behaviour of PP structures.

ELASTIC PLASTIC FRACTURE MECNANICS

The J integral as a failure criterion

The *J*-integral on any path Γ surrounding the crack tip is defined as

$$J=\int_{\Gamma}\left(w\mathrm{d}y-T\frac{\partial u}{\partial x}\mathrm{d}s\right) \tag{1}$$

where w is the strain energy density, T is the traction vector, $\partial u/\partial x$ is the displacement gradient, and s is the arc length[3]. It can be represented equally well by

$$J=-\frac{\partial U}{B\partial a} \tag{2}$$

i.e., the negative change in potential energy, U, per unit thickness (B) for an incremental change in crack length, a. That is, J is proportional to the area between the load–displacement curves of specimens with cracks of length a and $(a+\mathrm{d}a)$, respectively (see *Figure 1*). Equation (2) can also be written as

$$J=\int_{0}^{P}\left(\frac{\partial\Delta}{\partial a}\right)_{P}\mathrm{d}P=-\int_{0}^{\Delta}\left(\frac{\partial P}{\partial a}\right)_{\Delta}\mathrm{d}\Delta \tag{3}$$

where Δ is the load point displacement and P the load per unit thickness. For conditions that satisfy LEFM $J=(1-\nu^2)K^2/E=G$, where K is the stress intensity, E is the modulus, ν is Poisson's ratio and G is the strain energy release rate.

Begley and Landes[4] proposed that the value of J at crack initiation J_c be a fracture criterion and showed it to be a material property for specimens that exhibit large amounts of plasticity before fracture. Hence, J_c can be used to characterize fracture in ductile materials and is known as the ductile fracture toughness, analogous to G_{Ic} in LEFM.

0032-3861/85/121963-08$03.00

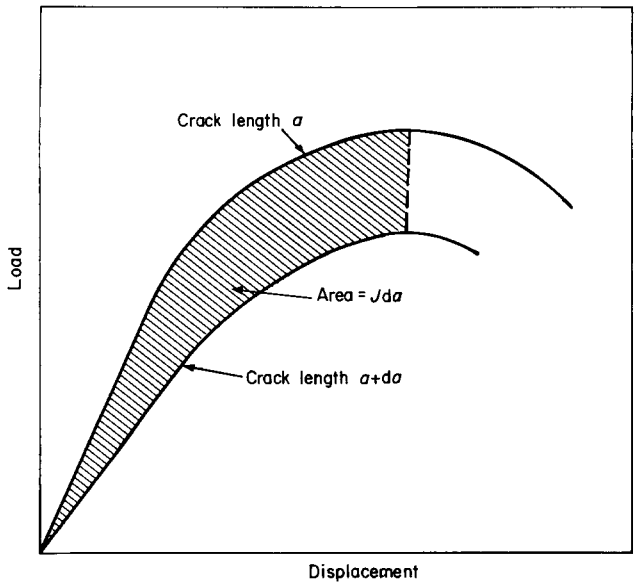

Figure 1 J determination from load–displacement curves for specimens with initial crack lengths of a and $a+da$. At initiation $J=J_c$

Schapery[9] theoretically justified the use of the J-integral as a failure criterion in non-homogenous, viscoelastic media. Chan and Williams[10] have recently used J to characterize fraction of polyethylene.

Tearing instability

Thus, J_c may provide a criterion for crack initiation in ductile polymers. However, nothing can be inferred about continued crack growth. A materials' resistance to crack extension beyond initiation (for $J>J_c$) can be characterized by the J *versus* Δa curve—the J-integral resistance curve. A typical curve is shown in *Figure 2*. The initial portion of this curve is due to the blunting of the crack tip[7] and is described by the equation

$$J=2\sigma_0\Delta a \tag{4}$$

where σ_0 is the flow stress for the material, defined as the average of the yield and tensile strength, and Δa is the average amount of crack growth. The latter portion of this curve is found to be approximately linear for ductile metals and the slope dJ/da is the tearing resistance and determines the stability of crack growth.

Paris *et al.*[7] introduced the concept of tearing instability (TIS) and the non-dimensional parameter, T, the tearing modulus

$$T=\frac{E}{\sigma_0^2}\left(\frac{\partial J}{\partial a}\right)$$

to describe the stability of crack growth and suggested it may be a material property.

Following Paris *et al.*[7] to illustrate the concept of TIS, consider a centre cracked specimen (CCS) as shown in *Figure 3*. The limit load P_L, the load at which the remaining ligament is fully plastic is

$$P_L=\sigma_0(W-2a)B \tag{5}$$

where W and B are the specimen width and thickness and $2a$ is the crack length. An increase in crack length by an amount da decreases the limit load by

$$dP_L=-2\sigma_0 B da \tag{6}$$

A decrease in load leads to elastic shortening, $d(\Delta_e)$, of the specimen by an amount

$$d(\Delta_e)=\frac{L dP_L}{WBE} \tag{7}$$

since

$$\frac{\Delta}{L}=\frac{\sigma}{E}=\frac{P}{EWB}$$

where L is the length of the specimen. From equations (6) and (7)

$$d(\Delta_e)=-\frac{2\sigma_0 L da}{WE} \tag{8}$$

Another effect of crack extension da is an increase in the plastic displacement, $d(\Delta_p)$, of the specimen, given by

$$d(\Delta_p)=\frac{dJ}{\sigma_0} \tag{9}$$

where dJ is the increase in the value of J required for crack extension da. Now, if the specimen was tested in a rigid machine (fixed grips), *instability* with rapid crack growth would ensue if the magnitude of elastic shortening $\frac{2\sigma_0 L da}{WE}$ exceeded the corresponding plastic lengthening $\frac{dJ}{\sigma_0}$ due to crack extension. From equations (8) and (9), the criterion for instability becomes

$$\frac{E}{\sigma_0^2}\frac{dJ}{da}<\frac{2L}{W} \tag{10}$$

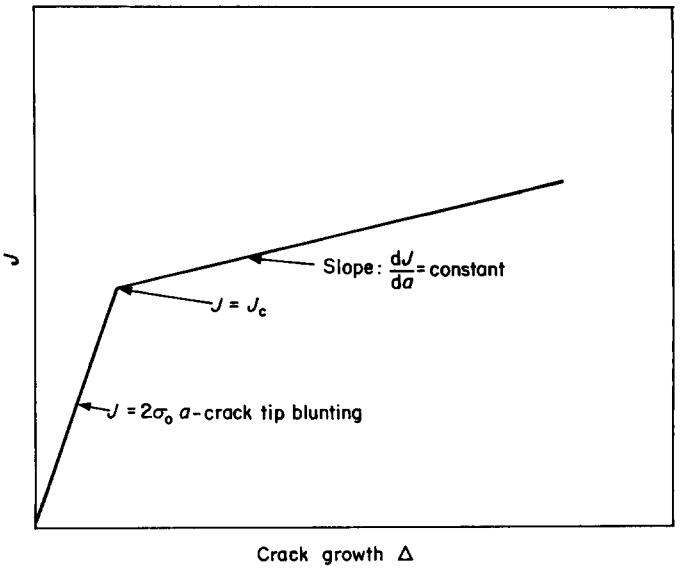

Figure 2 Schematic J resistance curve

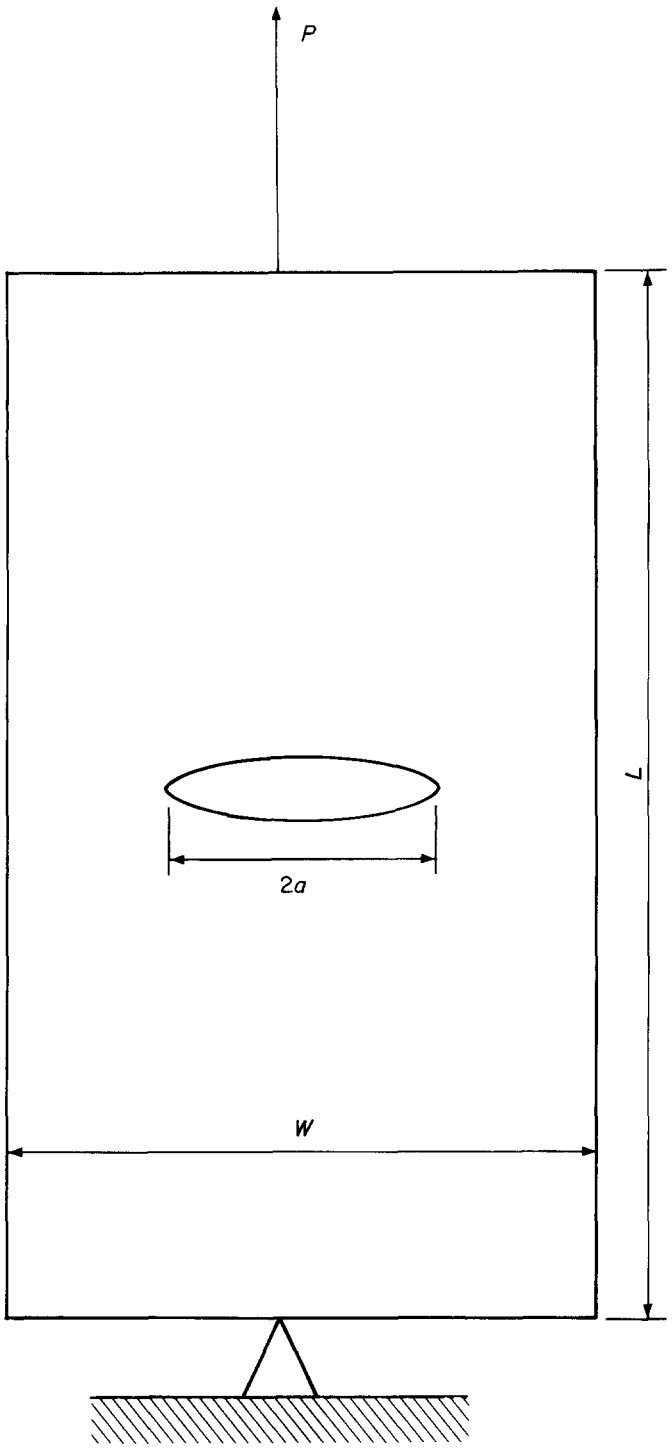

Figure 3 Centre cracked specimens

Paris *et al.* defined the left hand side of the inequality as the tearing modulus T_m and predicted it to be a material constant. The right hand side of the inequality in equation (10) is defined as T_a—a non-dimensional parameter governed by specimen geometry and loading configuration. T_a's for other specimen geometries are given in *Table 1*.

Determination of J *and* T_m

The following is a summary of the analysis of Ernst *et al.*[11] to determine J, T_m from three point bend (TPB) and compact tension (CT) specimens. J (equation (3)) can be divided into elastic and plastic parts J_e and J_p by dividing Δ into its elastic and plastic components Δ_e and Δ_p to give

$$J=\int_0^P\left(\frac{\partial\Delta_e}{\partial a}\right)_P dP+\int_0^P\left(\frac{\partial\Delta_p}{\partial a}\right)_P dP \tag{11}$$

The first term, the elastic part, is the Griffith strain energy release rate G.

Then, using the identity in equation (3)

$$J=G-\int_0^{\Delta_p}\left(\frac{\partial P}{\partial a}\right)_{\Delta_p} d\Delta_p \tag{12}$$

For plasticity confined to the remaining ligament, b, the following relationship for P as a function of Δ_p and a ($a=W-b$) can be written

$$P=\frac{b^2}{W}F_1\left(\frac{\Delta_p}{W}\right) \tag{13}$$

where W is the width of the specimen and F_1 is a calibration function that must be determined experimentally from the load as a function of the plastic displacement. Therefore,

$$J=G+\frac{2b}{W}\int_0^{\Delta_p}F_1\left(\frac{\Delta_p}{W}\right)d\Delta_p \tag{14}$$

Thus far the analysis assumes no crack growth. To extend this analysis for crack growth, integration of the total differential of equation (14) gives

$$J=G+\frac{2b}{W}\int_0^{\Delta_p}F_1 d\Delta_p+\int_{a_0}^{a}\frac{1}{b}\left(\frac{-2b}{W}\int_0^{\Delta_p}F_1 d\Delta_p\right)da \tag{15}$$

To obtain T_m, da must be determined by differentiating equation (13) and since $db=-da$

$$da=\frac{b^2}{W^2}\frac{\partial F_1}{\partial\left(\frac{\Delta_p}{W}\right)}d\Delta_p-dP\Big/\frac{2b}{W}F_1 \tag{16}$$

Therefore, from equations (14) and (16)

$$T_m=\frac{E}{\sigma_0^2}\left\{\frac{dG}{da}+\left[\left(\frac{2b}{W}F_1\right)^2\Big/\frac{b^2}{W^2}\frac{\partial F_1}{\partial\frac{\Delta_p}{W}}-\frac{dP}{d\Delta_p}\right]-\frac{2}{W}\int_0^{\Delta_p}F_1 d\Delta_p\right\} \tag{17}$$

Table 1 T applied for various specimens

Specimen	Loading	T_a
1 Centre cracked strip	Tension	$\frac{2L}{W}$
2 Double edge notched	Tension	$\frac{12L}{W}$
3 Three point bend	Bending	$\frac{2b^2S}{W^3}$
4 Compact tension specimen	Bending	Negative—hence always stable

0032-3861/85/121971-08$03.00

Once F_1 is known as an explicit function, then T_m, Δa and J can be determined. F_1 can be determined from the load displacement curves of sub-size or possibly full size specimens up to the point of crack initiation. From the load–displacement curve of these specimens, an F_1 *versus* $\frac{\Delta_p}{W}$ plot can be made, with $F_1 = \frac{PW}{b_0^2}$ and Δ_p, the plastic part of the total displacement. An expression can then be found to fit the F_1 *versus* $\frac{\Delta_p}{W}$ curve to give F_1 as an explicit function. Lin and co-workers[12] suggested a two-parameter fit for this function of the form

$$F_1 = F_0\left(\Delta_p W\right)^n \tag{18}$$

that can be substituted into equations (15), (16) and (17) to determine J, Δa and T_m explicitly. G and $\frac{dG}{da}$ can be obtained directly from LEFM[13]. The relations for TPB and CT specimens are given in Appendix A.

The load displacement curve of a full-size specimen beyond crack initiation (maximum load) can now be used along with equations (15)–(17) to determine Δa, J and T_m. dP and $d\Delta_p$ in equations (15) and (17) refer to an incremental drop in load and increase in plastic displacement upon crack growh, da, respectively.

The experimental steps involved in estimating Δa, J and T_m are summarized graphically in *Figure 4*. From the load–displacement curve of a cracked specimen but with no crack growth, P as a function of Δ_p is determined as shown in *Figure 4*. From a log–log plot of this data, the best fit representation is determined in terms of F_0 and n. Then dP and $d\Delta_p$ are determined beyond crack initiation and substituted into equations (15)–(17) to determine Δa, J and T_m.

(i) From load per unit thickness–displacement curves for sub-size (or full size) specimens up to crack initiation determine $F_1 = pW/b_2$ vs. $\Delta p/w$

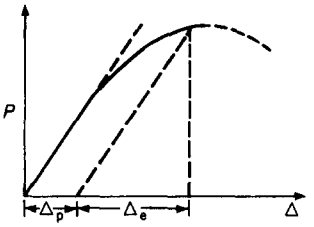

(ii) From log–log plot of F_1 vs. p/w, determine best fit values of F_0 and n for $F_1 = F_0(\Delta p/w)$

(iii) Obtain P vs. Δp for full size specimen, dP and Δ_p beyond crack initiation

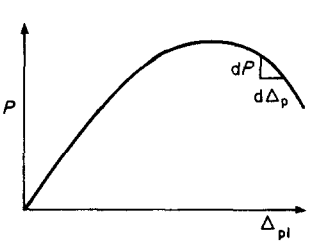

(iv) With incremental values of dP and $d\,P$ after crack initiation and equations (15)–(17) determine J, Δa and T_m

Figure 4 Summary of experimental steps to determine J, Δa and T_m

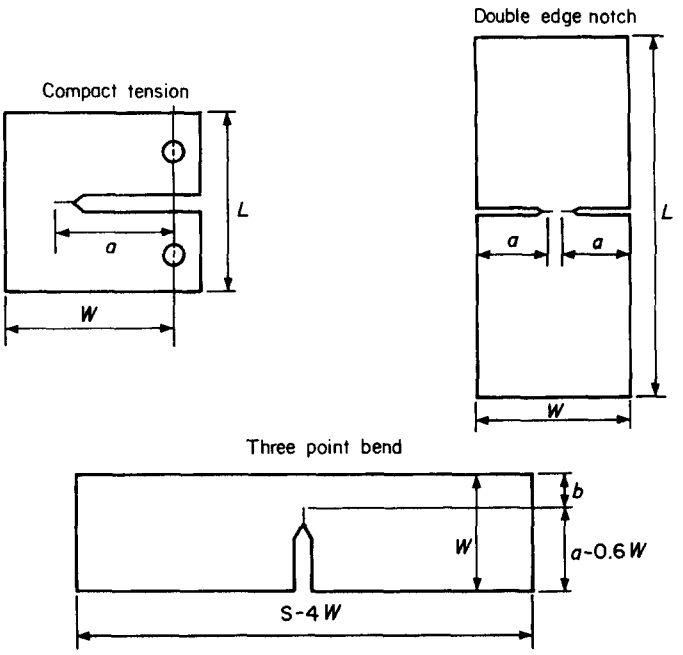

Figure 5 Types of fracture specimens used

MATERIALS AND PROCEDURES

Commercial PP (Westlake Plastics Co.) 12.5 mm thick was machined into tensile, sub- and full-sized TPB, CT and double edge notched DEN specimens. This thickness ensures plane strain conditions as determined by ASTM E 399[14]. *Figure 5* shows the dimensions of the fracture specimens. The PP was 45% crystalline, its melting point was 168°C and glass transition temperature (T_g) was −28°C from d.s.c.; it was isotactic, had a weight average molecular weight of 340000 and a number average molecular weight of 90000 and a spherulite size of about 0.2 mm.

After machining, the specimens were annealed at 150°C for 1 h to relieve any residual stresses and furnace cooled; then a razor cut was introduced at the base of the machined notch.

The mechanical tests on the tensile and fracture specimens were carried out at 23±2°C and relative humidity of 45±5% at four displacement rates $\dot{\Delta}$: 10^{-4}, 5×10^{-4}, 5×10^{-3} and 10^{-2} m min^{-1}.

T_m was evaluated by measuring the necessary parameters in CT and TPB specimens and the stability of crack growth in CT, TPB and double edge notch (DEN) specimens as a function of geometry.

RESULTS

The experimental data needed to evaluate TIS are E, σ_0, F_0, n, $d\Delta_p$ and dP. These data were determined at the four displacement rates. Then T_m was calculated from data obtained with tensile, CT, TPB specimens and the prediction of TIS in DEN specimens based on these data was tested. Also, the ductile fracture toughness, J_m (J at maximum load) was determined in CT and TPB specimens as a function of displacement rate. In this work, crack initiation was assumed to occur at or close to maximum load and hence J_m is used to estimate toughness, J_c.

Tensile properties. The modulus, E, determined from the initial portion of the stress–strain curve, the yield stress (at

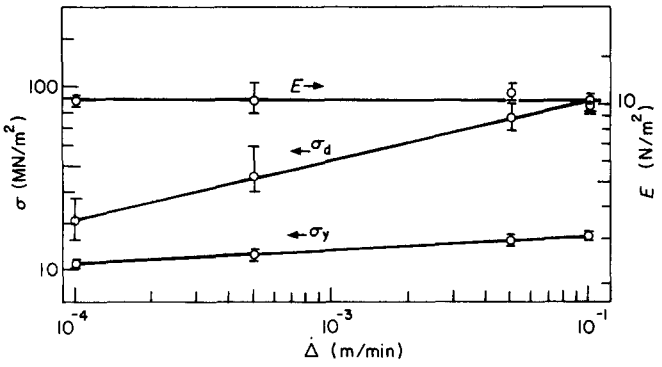

Figure 6 E, σ_y and σ_d as a function of displacement rate from conventional tensile tests

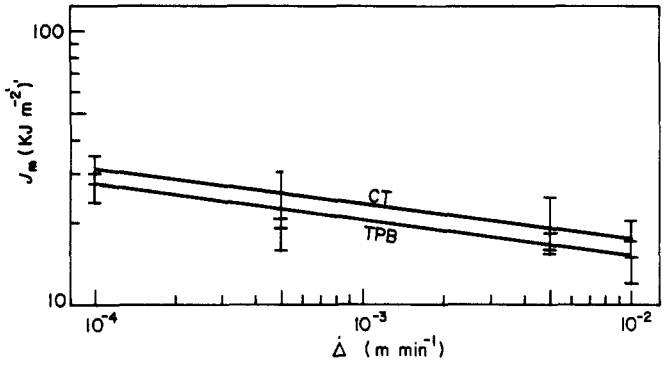

Figure 7 Variation in J_m with $\dot{\Delta}$ for TPB and CT specimens

maximum load), σ_y, and the true draw stress (at necking), σ_d, as a function of deformation rate, are shown in *Figure 6*. The modulus was independent of deformation rate over this relatively small deformation rate range, but the characteristic stresses increased as expected.

Fracture toughness. The fracture toughness was estimated by computing J_m at the maximum load in the load–deflection curve for the TBP and CT specimens as a function of strain rate (*Figure 7*). It was nearly independent of geometry and decreased with increasing deformation rate.

Tearing modulus. The tearing modulus was determined from the load–deflection curves of the TPB and CT specimens by determining the constants F_0 and n in equation (18) from the relationship of the applied load and resulting plastic displacement.

Figure 8 is a plot of F_1 *versus* Δ_p/W on a log–log scale for several deformation rates that shows this is a good representation of the data. F_0 and n were also determined from load–deflection curves of full-size CT specimens. The data for at least four specimens at each deformation rate are plotted for both types of specimens on *Figure 9*. F_0 was the same for both specimens and increased slightly with the deformation rate; n, however, for the TPB specimen was three times greater than that for the CT specimens and was independent of deformation rate for both types of specimens.

Once F_1 is known, T_m can be determined according to the following relationship

$$T_m = \frac{E}{\sigma_d^2}\left[\mathrm{d}G/\mathrm{d}a + \left\{\left[\frac{2b_0}{W}F_0\left(\frac{\Delta_p}{W}\right)^n\right]^2\right\}\Big/\left\{\frac{b_0^2}{W^2}F_0 n\left(\frac{\Delta_p}{W}\right)^{n-1} - \frac{\mathrm{d}P}{\mathrm{d}\Delta_p}\right\} - \frac{2F_0}{n+1}\left(\frac{\Delta_p}{W}\right)^{n+1}\right]$$

where G is the energy release rate from linear elastic fracture mechanics, a is the crack length, b_0 is the initial remaining ligament, and $\frac{\mathrm{d}P}{\mathrm{d}\Delta_p}$ is determined after crack growth is initiated (assumed to initiate at the maximum load). Instead of using σ_0 in the calculation of T_m, σ_d was used because the process zone in front of the crack tip stress whitens similarly to what happens during necking of a tensile specimen for which σ_d was the characteristic stress. T_m was calculated for TPB and CT specimens using this relationship and the data as a function of displacement rate are shown in *Figure 10*. T_m decreased with displacement rate for both types of specimens, but was about two times greater for the CT specimen than for the TPB specimen.

According to the theory, unstable tearing occurs when the tearing modulus $T_m < T_a$, where T_a is a non-dimensional parameter dependent on specimen geometry and the compliance of the system (*Table 1*).

T_a for CT specimens is always negative; therefore, CT specimens should always exhibit stable tearing. All CT

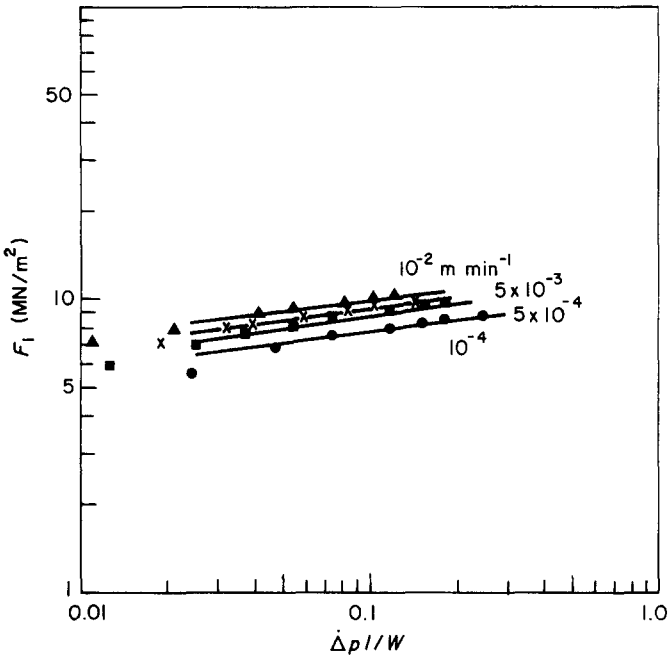

Figure 8 The calibration function F_1 ($\Delta pl/W$) for various displacement rates

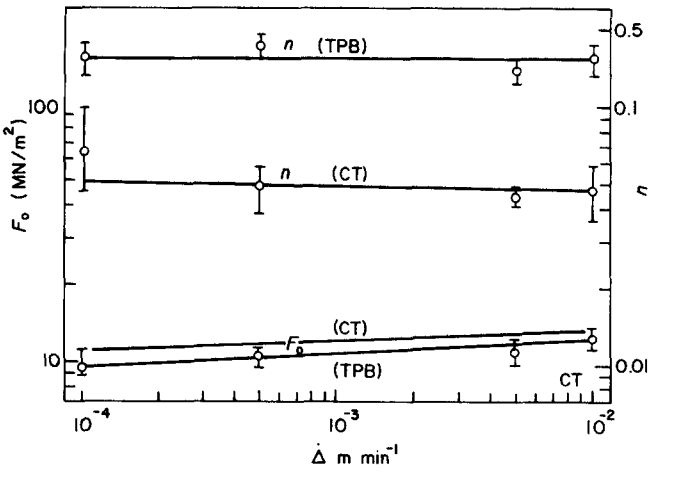

Figure 9 F_0 and n as a function defection rate for CT and TPB specimens

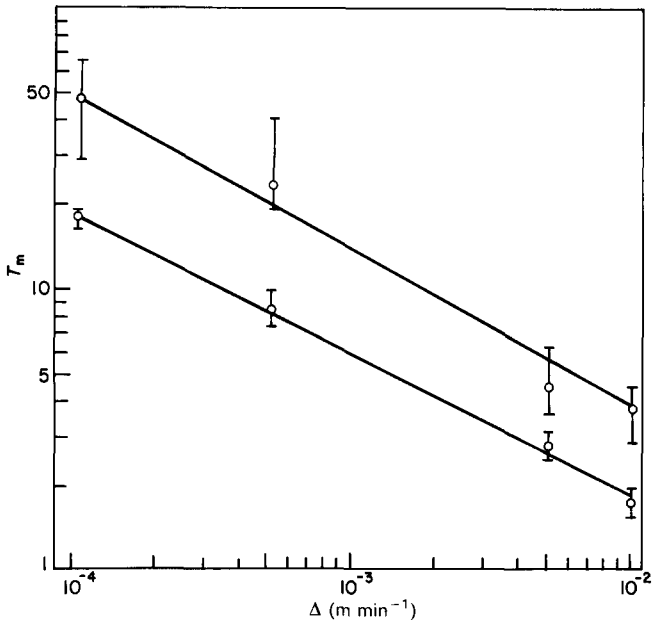

Figure 10 Variation in T_m with deflection rate for CT and TPB specimens

specimens at all deformation rates failed by stable crack growth.

T_a for TPB specimens depends on the geometry of the specimen and is given approximately by

$$T_a = \frac{2b^2 S}{W^3}$$

where S is the span length (see *Figure 5*). There should be a small additional term[15], but it has been neglected in this study. Therefore, increasing S, decreasing W or both increases the tendency towards instability. Tests were done by varying the dimensions to determine if the condition for instability was predicted by the measured values of T_m and calculated values of T_a in TPB specimens. *Table 2* gives the specimens' dimensions, deformation rate, T_a, T_m and whether fracture was stable or unstable. At the two lowest strain rates, fracture was stable as predicted since $T_a < T_m$, but at the highest strain rate, 10^{-2} m min^{-1}, all specimens were unstable even though T_a was less than T_m for four of the specimens tested. At 5×10^{-3} m min^{-1} the specimen for which $T_a = 1.3$ was less than $T_m = 2.8$ also failed in an unstable manner.

DEN specimens were tested at three deformation rates with different lengths to determine requirements for instability. For DEN specimens, $T_a = \frac{12L}{W}$. *Table 3* gives the results and *Figure 11* shows the load–deflection curves at $\dot{\Delta} = 10^{-4}$ m min^{-1} for specimens of different lengths and, therefore, different T_a's.

Figure 12 summarizes the results of the tearing instability for TPB and DEN specimens. The $T_m = T_a$ line theoretically distinguishes stable from unstable behaviour.

FRACTOGRAPHY

The fracture surfaces were radically different in the slow and fast crack growth regions, as shown in *Figure 13*. The morphology of the last fracture region did not change with deformation rate. The general morphology of the slow crack growth regions also remained the same with deformation rate, but was coarser at slower deformation rates.

Table 2 Tearing in three point bend specimens

$\dot{\Delta}$ (m min^{-1})	S (cm)	W (cm)	T_a	T_m	Failure mode
10^{-4}	10	2.5	1.6	18	S
10^{-4}	35	2.5	5.7	18	S
5×10^{-4}	7.6	2.5	1.2	8.5	S
5×10^{-4}	15	2.5	2.9	8.5	S
5×10^{-3}	10	6.4	0.3	2.8	S
5×10^{-3}	10	2.5	1.3	2.8	U
10^{-2}	13	10	0.2	1.7	U
10^{-2}	15	11	0.3	1.7	U
10^{-2}	23	10	0.2	1.7	U
10^{-2}	23	10	0.6	1.7	U
10^{-2}	18	2.5	3.5	1.7	U

S = Stable; U = Unstable

Table 3 Tearing in double edge notch specimens

$\dot{\Delta}$ (m min^{-1})	L (cm)	W (cm)	T_a	T_m	Failure mode
10^{-4}	4.3	5	10	18	S
10^{-4}	6.6	5	16	18	S
10^{-4}	8.9	5	21	18	U
10^{-4}	15	5	36	18	U
10^{-4}	30	5	72	18	U
5×10^{-4}	25	5	6	8.5	S
5×10^{-4}	50	5	12	8.5	U
5×10^{-4}	76	5	18	8.5	U
5×10^{-3}	1.3	5	3	2.8	U
5×10^{-3}	12.7	5	30	2.8	U

S = Stable; U = Unstable

DISCUSSION

Gotham and Scrutton's results[7] showing that CT specimens failed by stable ductile tearing but centre cracked specimens failed by unstable rapid crack growth motivated this study of TIS in PP. The results show that Paris *et al.*'s theory of TIS explains their results. From the dimensions of their specimens, T_a was 1.6 and at the deformation rate of their test, T_m would be about 1. Therefore, TIS theory predicts that the centre cracked specimens would exhibit unstable crack growth. But the CT specimens, since T_a is always negative, would fail by stable crack growth.

Likewise, TIS theory explains most of the results of this study. However, two of the results need further study and clarification.

(1) T_m was not independent of geometry and
(2) unstable fracture occurred at the higher deformation rates even though T_m was greater than T_a.

T_m determined from data obtained from CT specimens was two times that obtained from TPB specimens (see *Figure 10*). J_m was the same for both specimens (see *Figure 7*) and can therefore be considered independent of geometry. The source of this difference may be identified with n the coefficient in the expression for the calibration function F_1 since F_0 was the same for both specimens. Because of the different plastic zones in the two specimens, the extent of plastic deformation as a function of load

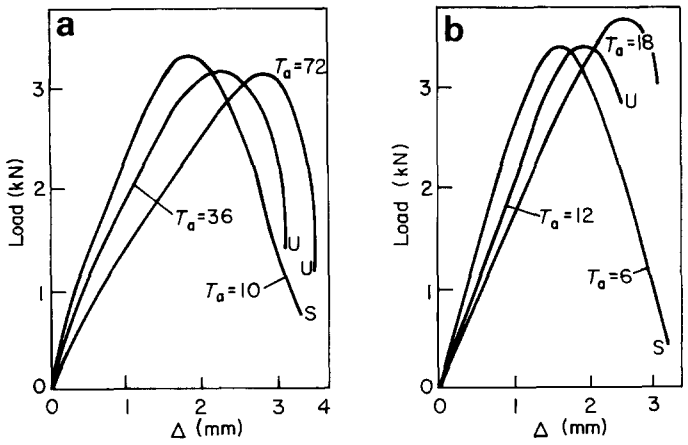

Figure 11 Load–displacement curves for double edge notched specimens at (a) 10^{-4} m min^{-1} and $T_m = 18$ and (b) 5×10^{-4} m min^{-1} and $T_m = 8.0$. S: stable; U: unstable

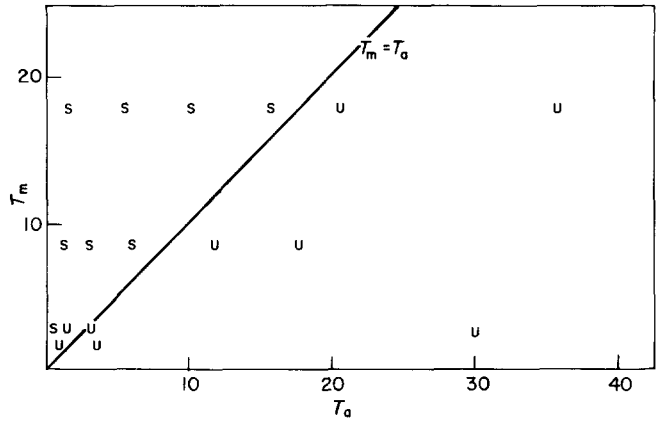

Figure 12 Summary of results; solid line divides stable from unstable crack propagation. S: stable; U: unstable

could be different and thus account for the different n's and T_m obtained. Other investigators studying metals have made similar observations[16] and consequently T_m is not independent of the geometry of the specimen and may not be a material property.

At the higher strain rates some specimens failed in an unstable way even though T_a was less than T_m, requiring some comment. A possible explanation is that as the deformation rate increases, the yield strength increases (see *Figure 6*) and therefore, the size of the plastic zone decreases and the remaining ligament was not fully plasticized. The values of T_a calculated were based on the assumption of full plasticity in the remaining ligament. Thus, the lack of full plasticity in the remaining ligament effectively increases T_a and unstable crack growth becomes probable.

Another manifestation of the effect of deformation rate on the extent of plasticity is the decrease of both J_m and T_m with increasing deformation rate. Because the extent of plasticity is reduced the critical crack driving force (J_m) and the resistance to crack growth (T_m) are decreased. These are not unexpected results.

Overall the theory of TIS explains many of the observations regarding the ductile fracture of PP previously unexplained and provides a basis for better characterization of the ductile fracture properties of polymers.

CONCLUSIONS

1 J_m was independent of specimen geometry, but T_m was not.
2 J_m and T_m decreased with deformation rate.
3 TIS theory explains the dependence of crack growth stability on geometry.

ACKNOWLEDGEMENTS

The authors wish to express their gratitude to Dr Jwo Pan of Battelle-Columbus Laboratories for helpful discussions of this work and the Materials Research Laboratory, University of Massachusetts, funded by the US National Science Foundation, for financial support.

APPENDIX A

$$G = \frac{K^2}{E} = \frac{1}{E}\frac{P^2 S^2}{B^2 W^3}\left[Y_1\left(\frac{a}{W}\right)\right]^2 \qquad \text{for TPB specimen}$$

and

$$= \frac{1}{E}\frac{P^2}{B^2 W}\left[Y_2\left(\frac{a}{W}\right)\right]^2 \qquad \text{for CT specimen}$$

where S is the span, B is the thickness, W is the width, a/W is the crack aspect ratio and

$$Y_1\left(\frac{a}{W}\right) = 2.9\left(\frac{a}{W}\right)^{0.5} - 4.6\left(\frac{a}{W}\right)^{1.5} + 21.8\left(\frac{a}{W}\right)^{2.5} - 37.6\left(\frac{a}{W}\right)^{3.5} + 38.7\left(aW\right)^{4.5}$$

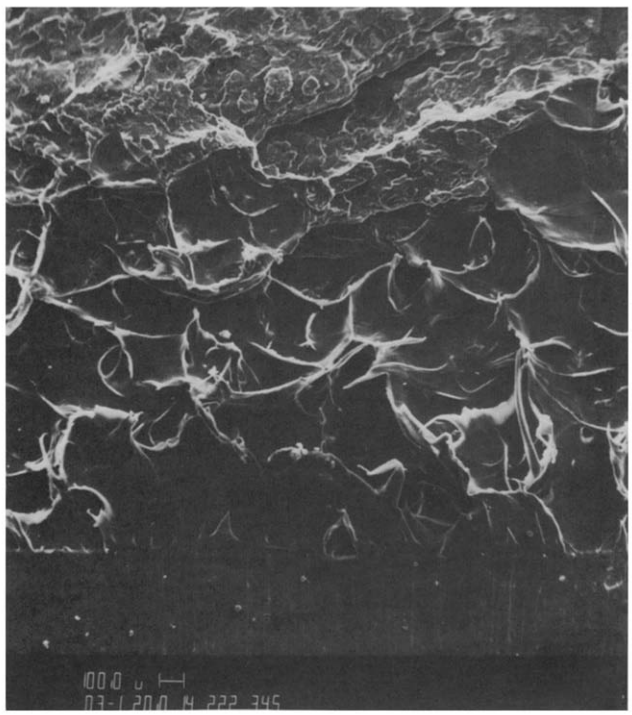

Figure 13 Fracture surface showing stable crack growth region (lower portion) and unstable region (upper portion)

$$Y_2\left(\frac{a}{W}\right)=29.6\left(\frac{a}{W}\right)^{0.5}-185.5\left(\frac{a}{W}\right)^{1.5}+655.7\left(\frac{a}{W}\right)^{2.5}-1017\left(\frac{a}{W}\right)^{3.5}+638.9\left(\frac{a}{W}\right)^{4.5}$$

REFERENCES

1 Friedrich, K. *Progr. Coll. Polym. Sci.* 1977, **64**, 103
2 Freidrich, K. *Progr. Coll. Polym. Sci.* 1979, **66**, 299
3 Rice, J. R. *J. Appl. Mech.* 1968, **35**, 379
4 Begley, J. A. and Landes, J. D. 'The *J*-Integral as a Fracture Criterion', *ASTM STP514*, American Society of Testing and Materials, Philadelphia, PA, pp. 1–20, 1972
5 ASTM Standard E813, 1982 Annual ASTM Standard, Part 10, pp. 822–840
6 Hodgkinson, J. M. and Williams, J. G. '*J* and G_c Analysis of the Tearing of a Highly Ductile Polymer', *J. Mater. Sci.* 1981, **16**, 50
7 Paris, P. C., Tada, H., Zahoor, A. and Ernst, H. *Elastic-Plastic Fracture*, ASTM STP 688, 1979, 5
8 Gotham, K. V. and Scrutton, I. N. *Polymer* 1978, **19**, 341
9 Schapery, R. A. *Fracture Mechanics* 1978, **XII**, 137
10 Chan, M. K. V. and Williams, J. G. *Int. J. Fract.* 1983, **19**, 145
11 Ernst, H., Paris, P. C., Rossow, M. and Hutchinson, J. W. *Fracture Mechanics*, ASTM STP 677, 1979, 581
12 Lin, I. H., Mirth, J. P. and Rosenfield, A. R. *Int. J. Fract.* 1980, **16**, R11
13 Knott, J. F. 'Fundamental Fracture Mechanics', Wiley, New York, 1973, 114
14 ASTM Standard E399, 1981 Annual ASTM Standard Part 10, pp. 588–618
15 Ernst, H. A., Paris, P. C. and Landes, J. D. 'Estimation of J-Integral and Tearing Modulus from a Single Specimen Record, *ASTM STP743*, pp. 476–502, 1981
16 Ernst, H. A. and Landes, J. D. 'Elastic-Plastic Fracture Mechanics Metholodology Using the Modified J, Jm Resistance Curve Approach', Westinghouse Scientific Paper No. 82-1D7-Metal, December 1982